Video Article

Fabrication of 3D Carbon Microelectromechanical Systems (C-MEMS)

Bidhan Pramanick[1], Sergio O. Martinez-Chapa[1], Marc Madou[1,2], Hyundoo Hwang[1,3]

[1]School of Engineering and Sciences, Tecnologico de Monterrey

[2]Department of Mechanical and Aerospace Engineering, University of California

[3]BBB Inc

Correspondence to: Hyundoo Hwang at hwang@itesm.mx

URL: https://www.jove.com/video/55649
DOI: doi:10.3791/55649

Keywords: Engineering, Issue 124, Carbon-MEMS/NEMS, glassy carbon, fabrication, lithography, pyrolysis, SU8, photoresist, human hair.

Date Published: 6/17/2017

Citation: Pramanick, B., Martinez-Chapa, S.O., Madou, M., Hwang, H. Fabrication of 3D Carbon Microelectromechanical Systems (C-MEMS). *J. Vis. Exp.* (124), e55649, doi:10.3791/55649 (2017).

Abstract

A wide range of carbon sources are available in nature, with a variety of micro-/nanostructure configurations. Here, a novel technique to fabricate long and hollow glassy carbon microfibers derived from human hairs is introduced. The long and hollow carbon structures were made by the pyrolysis of human hair at 900 °C in a N_2 atmosphere. The morphology and chemical composition of natural and pyrolyzed human hairs were investigated using scanning electron microscopy (SEM) and electron-dispersive X-ray spectroscopy (EDX), respectively, to estimate the physical and chemical changes due to pyrolysis. Raman spectroscopy was used to confirm the glassy nature of the carbon microstructures. Pyrolyzed hair carbon was introduced to modify screen-printed carbon electrodes ; the modified electrodes were then applied to the electrochemical sensing of dopamine and ascorbic acid. Sensing performance of the modified sensors was improved as compared to the unmodified sensors. To obtain the desired carbon structure design, carbon micro-/nanoelectromechanical system (C-MEMS/C-NEMS) technology was developed. The most common C-MEMS/C-NEMS fabrication process consists of two steps: (i) the patterning of a carbon-rich base material, such as a photosensitive polymer, using photolithography; and (ii) carbonization through the pyrolysis of the patterned polymer in an oxygen-free environment. The C-MEMS/NEMS process has been widely used to develop microelectronic devices for various applications, including in micro-batteries, supercapacitors, glucose sensors, gas sensors, fuel cells, and triboelectric nanogenerators. Here, recent developments of a high-aspect ratio solid and hollow carbon microstructures with SU8 photoresists are discussed. The structural shrinkage during pyrolysis was investigated using confocal microscopy and SEM. Raman spectroscopy was used to confirm the crystallinity of the structure, and the atomic percentage of the elements present in the material before and after pyrolysis was measured using EDX.

Video Link

The video component of this article can be found at https://www.jove.com/video/55649/

Introduction

Carbon has many allotropes and, depending on the particular application, one of the following allotropes can be chosen: carbon nanotubes (CNTs), graphite, diamond, amorphous carbon, lonsdaleite, buckminsterfullerene (C_{60}), fullerite (C_{540}), fullerene (C_{70}), and glassy carbon[1,2,3,4]. Glassy carbon is one of the most widely used allotropes because of its physical properties, including high isotropy. It also has the following properties: good electrical conductivity, low thermal expansion coefficient, and gas impermeability.

There has been a continuous search for carbon-rich precursor materials to obtain carbon structures. These precursors can be manmade materials or natural products that are available in particular shapes, and even include waste products. A wide variety of micro/nanostructures are formed via biological or environmental processes in nature, resulting in unique features that are extremely difficult to create using conventional manufacturing tools. As patterning took place naturally in this case, the synthesis of nanomaterials using natural and waste hydrocarbon precursors could be carried out using an easy, one-step process of thermal decomposition in an inert or vacuum atmosphere, called pyrolysis[5]. High-quality graphene, single-walled CNTs, multi-walled CNTs, and carbon dots have been produced by thermal decomposition or the pyrolysis of plant-derived precursors and wastes, including seeds, fibers, and oils, such as turpentine oil, sesame oil, neem oil (*Azadirachta indica*), eucalyptus oil, palm oil, and jatropha oil. Also, camphor products, tea-tree extracts, waste foods, insects, agro wastes, and food products have been utilized[6,7,8,9] Recently, researchers have even used silk cocoons as a precursor material to prepare porous carbon microfibers[10]. Human hair, usually considered a waste material, was recently used by this team. It is made up of approximately 91% polypeptides, which contain more than 50% carbon; the rest are elements such as oxygen, hydrogen, nitrogen, and sulphur[11]. Hair also comes with several interesting properties, such as very slow degradation, high tensile strength, high thermal insulation, and high elastic recovery. Recently, it has been used to prepare carbon flakes employed in supercapacitors[12] and to create hollow carbon microfibers for electrochemical sensing[13].

The machining of a bulk carbon material to fabricate three-dimensional (3D) structures is a difficult task, as the material is very brittle. Focused ion beam[14,15] or reactive ion etching[16] may be useful in this context, but they are expensive and time-consuming processes. Carbon microelectromechanical system (C-MEMS) technology, which is based on the pyrolysis of patterned polymeric structures, represents a versatile alternative. In the past two decades, C-MEMS and carbon nanoelectromechanical systems (C-NEMS) have received much attention because of

the simple and inexpensive fabrication steps involved. The conventional C-MEMS fabrication process is carried out in two steps: (i) patterning a polymer precursor (*e.g.,* a photoresist) with photolithography and (ii) pyrolysis of the patterned structures. Ultraviolet (UV)-curable polymer precursors, such as SU8 photoresists, are often used to pattern structures based on photolithography. In general, the photolithography process includes steps for spin coating, soft bake, UV exposure, post bake, and development. In the case of C-MEMS; silicon; silicon dioxide; silicon nitride; quartz; and, more recently, sapphire have been used as substrates. The photo-patterned polymer structures are carbonized at a high temperature (800-1,100 °C) in an oxygen-free environment. At those elevated temperatures in a vacuum or inert atmosphere, all of the non-carbon elements are removed, leaving only carbon. This technique allows for the attainment of high-quality, glassy carbon structures, which are very useful for many applications, including electrochemical sensing[17], energy storage[18], triboelectric nanogeneration[19], and electrokinetic particle manipulation[20]. Also, the fabrication of 3D microstructures with high aspect ratios using C-MEMS has become relatively easy and has led to a wide variety of carbon electrodes applications[18,21,22,23], often replacing noble metal electrodes.

In this work, the recent development of a simple and cost-effective way to fabricate hollow carbon microfibers from human hair using non-conventional C-MEMS technology[13] is introduced. The conventional SU8 polymer-based C-MEMS process is also described here. Specifically, the fabrication procedure for high-aspect ratio solids and hollow SU8 structures is described[24].

Protocol

1. 3D Human Hair-derived Carbon Structure Fabrication

NOTE: Use personal protective equipment. Follow laboratory instructions to use the instruments and to work inside the laboratory.

1. Prepare collected human hair by washing it with DI water and drying it with N_2 gas.
2. Arrange the hairs as desired, such as in parallel strands, cross over, with two hairs wound together, *etc.*
3. Attach the hairs to a silicon substrate using SU8 or keep them directly in a ceramic boat.
4. Place the hair-attached silicon substrate or boat into a furnace.
5. Turn on the furnace and open the valve of an inert gas (N_2) tank.
   NOTE: The optimal gas flow rate is dependent upon the volume of the furnace tube. A 6 L/min flow rate was applied for a tube volume of 6 L. To establish a completely inert environment in the furnace tube, a gas flow rate 1.5 times higher than the optimal gas flow rate was applied for the first 15 min.
6. **Set the parameters, including maximum pyrolysis temperature, temperature ramp rate, and inert gas flow rate, and run the furnace.**
   1. For example, increase temperature from room temperature to 300 °C at a 5 °C/min ramp rate. Keep it at 300 °C for 1 h for stabilization. Further increase the temperature to 900 °C and maintain it for 1 h more for carbonization.
   2. Cool the furnace down to 300 °C at a rate of 10 °C/min and turn off the heater of the furnace, as the controlled cooling is not necessary after 300 °C. Leave the samples in the furnace until the temperature reaches room temperature by N_2 flow only.
7. Turn off the furnace and gas flow upon the completion of the pyrolysis process.
8. Take the samples out of the furnace.

2. 3D Polymer Structure Fabrication: Photolithography

1. Design a 2D layout of the desired 3D photoresist structure using an appropriate software package and prepare the printed mask (*i.e.,* a polyethylene photofilm mask).
   NOTE: A commercial service was used to get the design printed. The size of the mask generally depends on the design.
2. In a clean laboratory facility, turn on two hot plates and set the temperatures to 65 °C and 95 °C, respectively.
3. Switch on a spin coater and a vacuum pump. Ensure that the vacuum pump is connected through a tube to the spinner head.
4. Set the parameters of the two-step spin, such as the spinning speed, ramp, and duration. For the first step, set the spinning speed to 500 rpm, the ramp to 100 rpm/s, and the spin time to 10 s to begin the spin cycle. For the next step, set the spinning speed to 1,000 rpm, the ramp to 100 rpm/s, and the spin time to 30 s to evenly spread the photoresist.
5. Place a substrate (*i.e.,* a 4 inch x 4 inch and 550 µm ± 25 µm-thick Si wafer with a 1 µm-thick SiO_2 layer) at the center of the holder.
6. Deposit photosensitive polymer *(i.e.,* SU8 photoresist) directly onto the center of the substrate. Use enough to cover the surface.
7. Push the "vacuum" button to hold the substrate.
8. Push the "run" button to coat the substrate with SU8 and to achieve a final thickness of 250 µm.
9. After the completion of spinning process, press the "vacuum" button again to release the coated substrate from the holder.
10. Hold the coated substrate carefully using a tweezer to keep the surface smooth and clean. Transfer the substrate directly onto the hot plate at 65 °C temperature for 6 min and then onto the hot plate at 95 °C temperature for 40 min (soft bake).
    NOTE: Baking at 65 °C is required to ensure the slow evaporation of the solvent, resulting in the better coating and better adhesion to the substrate, while baking at 95 °C further densifies the SU8.
11. In the meantime, press the switch to turn on the UV-exposure system and set the time of exposure to "12 s" using the set button in the system.
    NOTE: For a 250 µm-thick SU8 layer, the exposure energy must be 360 mJ/cm^2.
12. Once the baking step (step 2.10) is completed, put the substrate into the UV-exposure system and place the printed side of a photomask (from step 2.1) onto it. Use the whole mask area to cover the coated substrate and press gently to ensure that there is no gap between the mask and substrate.
13. Expose the SU8-coated substrate to UV radiation through the photomask using predefined UV settings.
14. Heat the substrate again by placing it directly on the hotplate at 65 °C for 5 min and at 95 °C for 14 min for a post-exposure bake (PEB).
    NOTE: The PEB increases the degree of cross-linking in the UV-exposed areas and makes the coating more resistant to solvents in the development step.

15. Remove the unexposed photoresist regions by dipping the substrate in the dedicated developer solution, placed in a beaker, for 20 min. Continuously shake the solution (carefully) to ensure the complete removal of the un-exposed resist areas.
16. Dry the developed structures by holding the substrate and blowing nitrogen or compressed air onto it.
17. Inspect the wafer under a microscope with 50X magnification to compare the patterns transferred to the photoresist with the desired patterns.

3. 3D Carbon Structure Fabrication: Pyrolysis

1. Place the samples prepared using photolithography (steps 2.1-2.17) inside a pressurized, open-ended tube furnace.
2. Turn on the furnace and set the parameters for pyrolysis, as mentioned above in step 1. Repeat the process from step 1.6-1.8.
3. Handle the samples carefully using tweezers and proceed to characterization.

Representative Results

A schematic of the fabrication process for human hair-derived hollow carbon microfibers is shown in **Figure 1**. The carbonized human hair was characterized using SEM to estimate the shrinkage. The hair diameter shrank from 82.88 ± 0.003 µm to 31.42 ± 0.003 µm due to the pyrolysis. Scanning electron microscopic (SEM) images of various patterns made using hair-derived carbon microfibers are shown in **Figure 2**. The atomic percentages of the elements present in the hair before and after pyrolysis are presented in **Table 1**. The human hair used in this research was (atomic percent) 66.57% carbon, 16.19% oxygen, 7.94% nitrogen, 9.14% sulphur, and a small percentage of minerals such as calcium. The atomic percentage of carbon and oxygen was found to be 80.84%, and 14.83% respectively after the pyrolysis. Raman spectroscopic analysis of the hair before and after pyrolysis was also performed as shown in **Figure 3**. Only two broad peaks corresponding to the D- and G-bands were found for the hair after pyrolysis. The ratio of the intensities of the D-band to the G-band in the hair-derived carbon fibers was calculated to be 0.99, indicating that the hair-derived fibers are mostly glassy carbon.

The hair-derived carbon fibers were applied to detect dopamine and ascorbic acid using an electrochemical sensor. A screen-printed carbon electrode was modified with the hair-derived carbon fibers and used as the working electrode of the sensor. A schematic diagram of the carbon electrodes for electrochemical sensing is shown in **Figure 4a**. Cyclic voltammograms of 100 µM dopamine and 100 µM ascorbic acid in a 0.1 M phosphate buffer solution of pH 7.4 are shown in **Figure 4b** and c, respectively. A bare carbon electrode, a carbon electrode modified with the hair-derived carbon, and a carbon electrode modified with the CNTs were used as the working electrode of the sensors to compare the performance to detect dopamine and ascorbic acid. The oxidation peaks for dopamine were measured at 333 mV for the bare carbon electrode, 266 mV for the carbon electrode modified with the hair derived carbon fibers, and 96 mV for the electrode modified with the CNTs. The oxidation peaks for ascorbic acid were observed at 414 mV, 455 mV, and 297 mV for those electrodes, respectively.

A schematic diagram of the conventional C-MEMS process, the photolithographic patterning of a polymer precursor and the subsequent pyrolysis, is shown in **Figure 5**. These fabricated structures were characterized using confocal microscopy and SEM to estimate the shrinkage due to pyrolysis. Five cylindrical structures of the same height (250 µm) and outer diameter (150 µm), but with various inner diameters (*i.e.,* 0 (solid), 30, 50, 75, and 100 µm (hollow)) were fabricated for this study. The geometric changes of the cylindrical structures due to pyrolysis were measured. The percentage of shrinkage was varied for different inner and outer diameter structures. When the inner diameter was 0 µm (a solid microstructure), the outer diameter shrank around 35%. When the the inner diameters were 30, 50, and 75 µm, the outer diameters and inner diameters shrank around 42% and 30 - 35%, respectively. In the case of a 100-µm inner diameter, the inner diameter expanded 12%, rather than shrinking, and the outer diameter shrank only 15%. In **Figure 6**, the SEM images of solid and hollow carbon microstructures, of which the original inner diameters were 30, 40, and 75 µm, are shown. 3D optical images of hollow microstructures before and after pyrolysis are also shown in **Figure 7**. All the microstructures shrank almost 30% in height (250 to 175 µm) according to the confocal microscopic images.

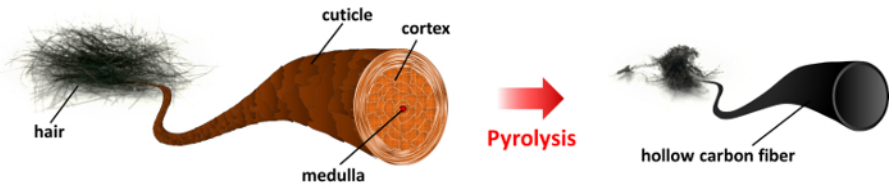

Figure 1: Schematic Diagram of the Fabrication Process for Human Hair-derived Hollow Carbon Microfibers. Reproduced with permission from reference[13]. Copyright 2016, Elsevier Ltd. Please click here to view a larger version of this figure.

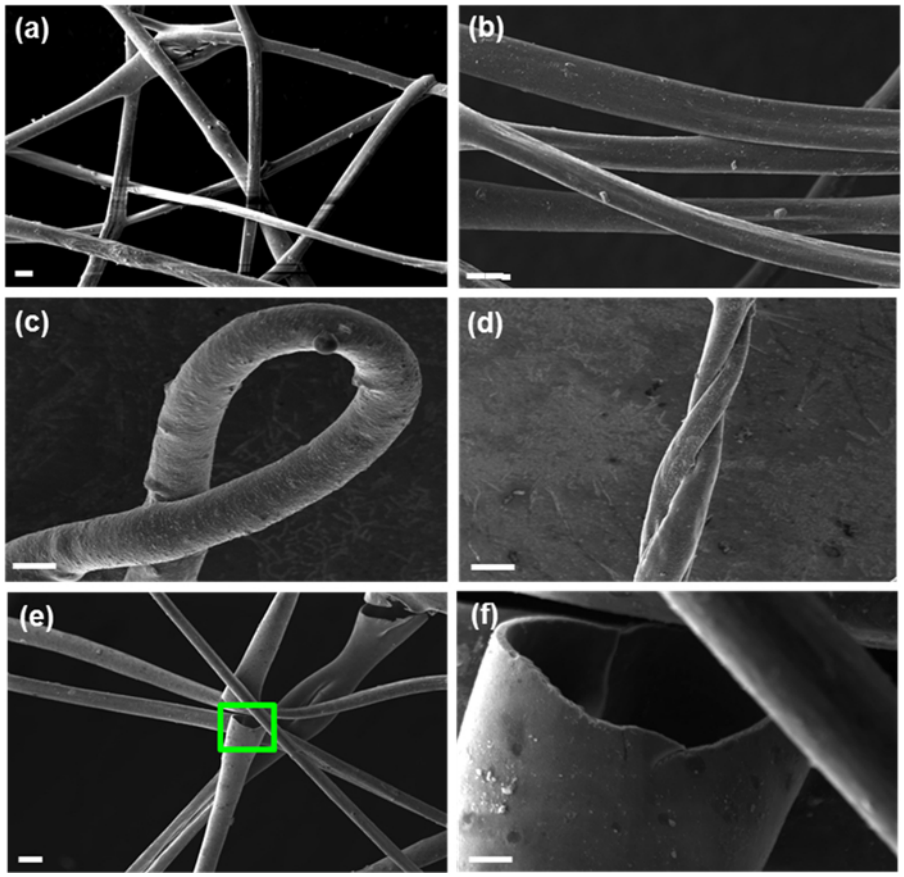

Figure 2: SEM Images of Different Patterns of Hair-derived Carbon Microfibers. (**a** and **b**) Aligned straight carbon microfibers. Scale bar = 50 µm. (**c** and **d**) A coiled carbon microfiber. Scale bars = 20 and 100 µm, respectively. (**e** and **f**) A broken hollow carbon microfiber**.** Reproduced with permission from reference[13]. Copyright 2016, Elsevier Ltd. Please click here to view a larger version of this figure.

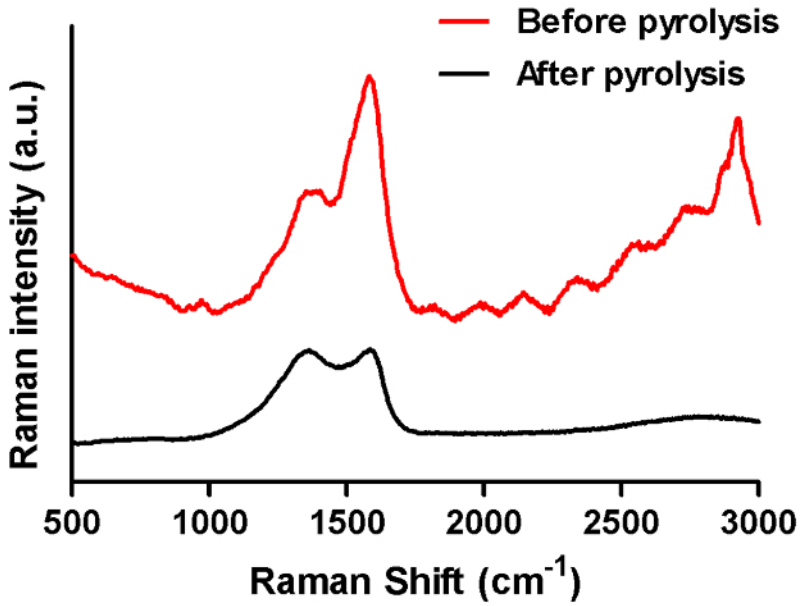

Figure 3: Raman Spectra of Human Hair Before and After Pyrolysis. Reproduced with permission from reference[13]. Copyright 2016, Elsevier Ltd. Please click here to view a larger version of this figure.

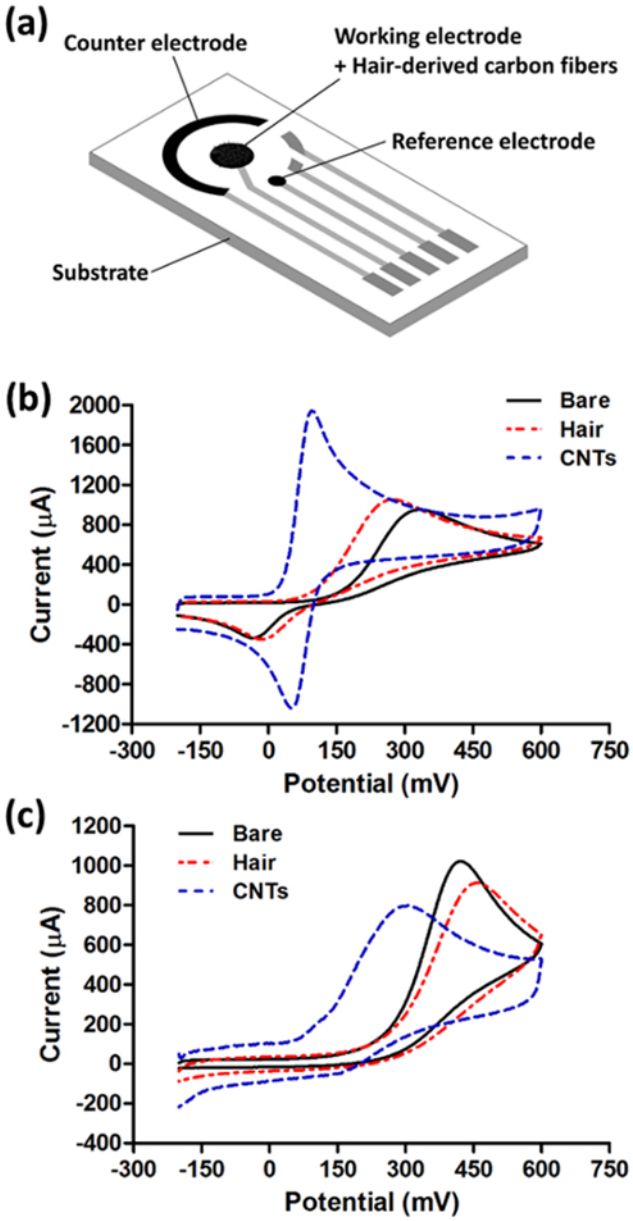

Figure 4: Electrochemical Sensing of Dopamine and Ascorbic Acid. (**a**) Schematic diagram of carbon electrodes for electrochemical sensing. Cyclic voltammograms of (**b**) 100 μM dopamine and (**c**) 100 μM ascorbic acid. Reproduced with permission from reference[13]. Copyright 2016, Elsevier Ltd. Please click here to view a larger version of this figure.

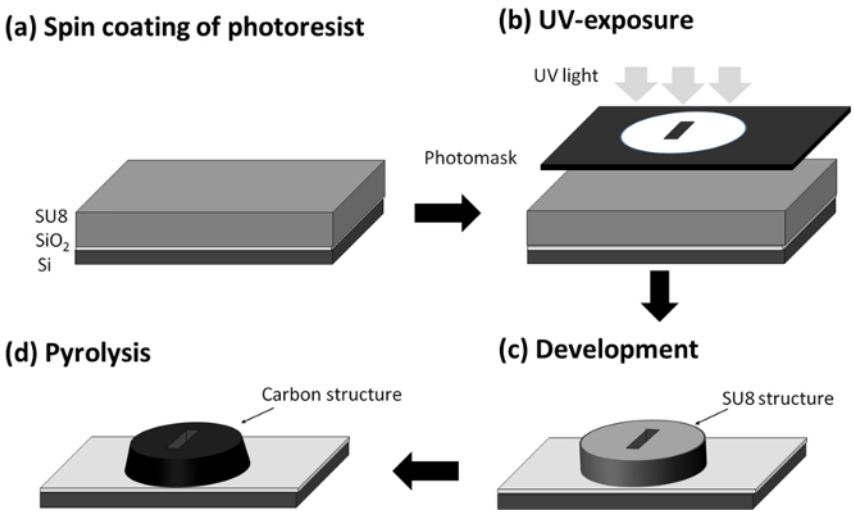

Figure 5: A Schematic Diagram of the Conventional C-MEMS Process Based on Photolithography and pyrolysis. (**a**) Spin coating of photoresist, (**b**) UV-exposure, (**c**) development, and (**d**) pyrolysis. Please click here to view a larger version of this figure.

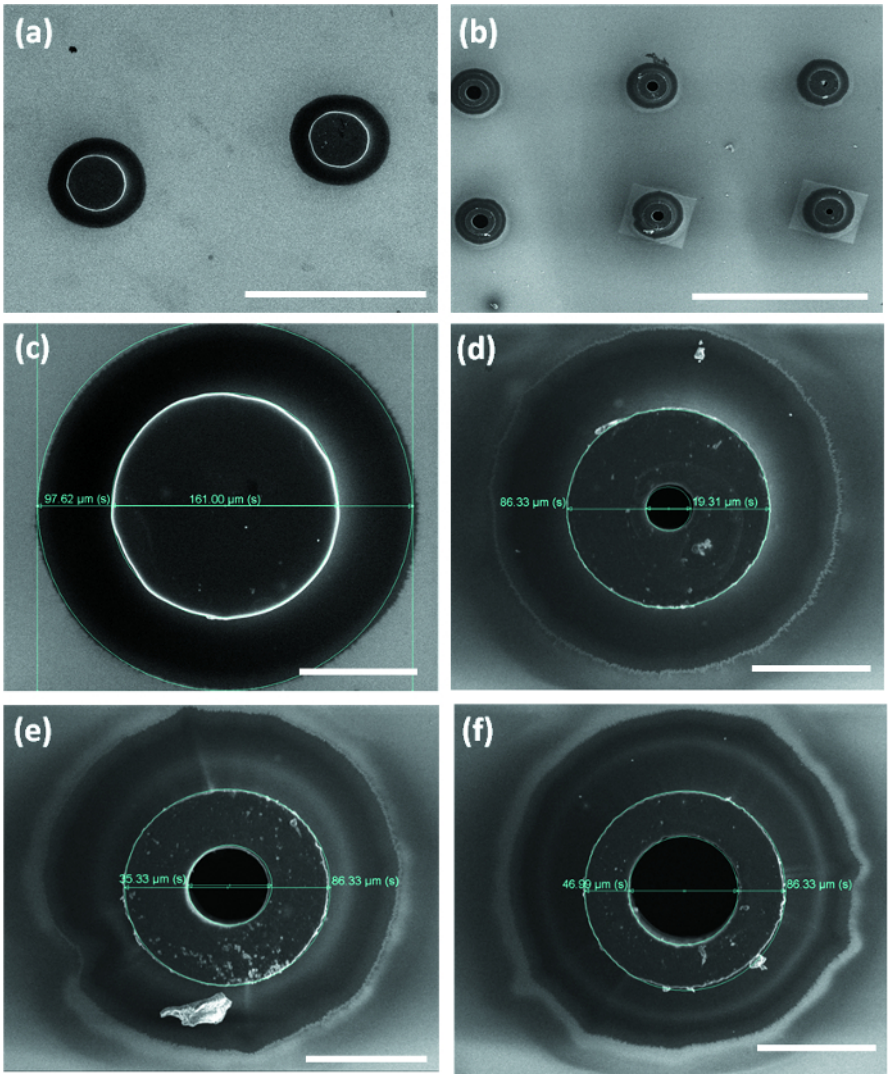

Figure 6: Scanning Electron Microscopic Images of Carbon Microstructures Fabricated by the Conventional C-MEMS Process. (**a**) Solid and (**b**) hollow structures with various inner diameters. Scale bars = 500 µm. Enlarged images for (c) the solid and the hollow structures, of which the inner diameters before pyrolysis were (**d**) 30, (**e**) 50, and (**f**) 75 µm. Scale bars = 50 µm. Reproduced with permission from reference[24]. Copyright 2016, The Electrochemical Society. Please click here to view a larger version of this figure.

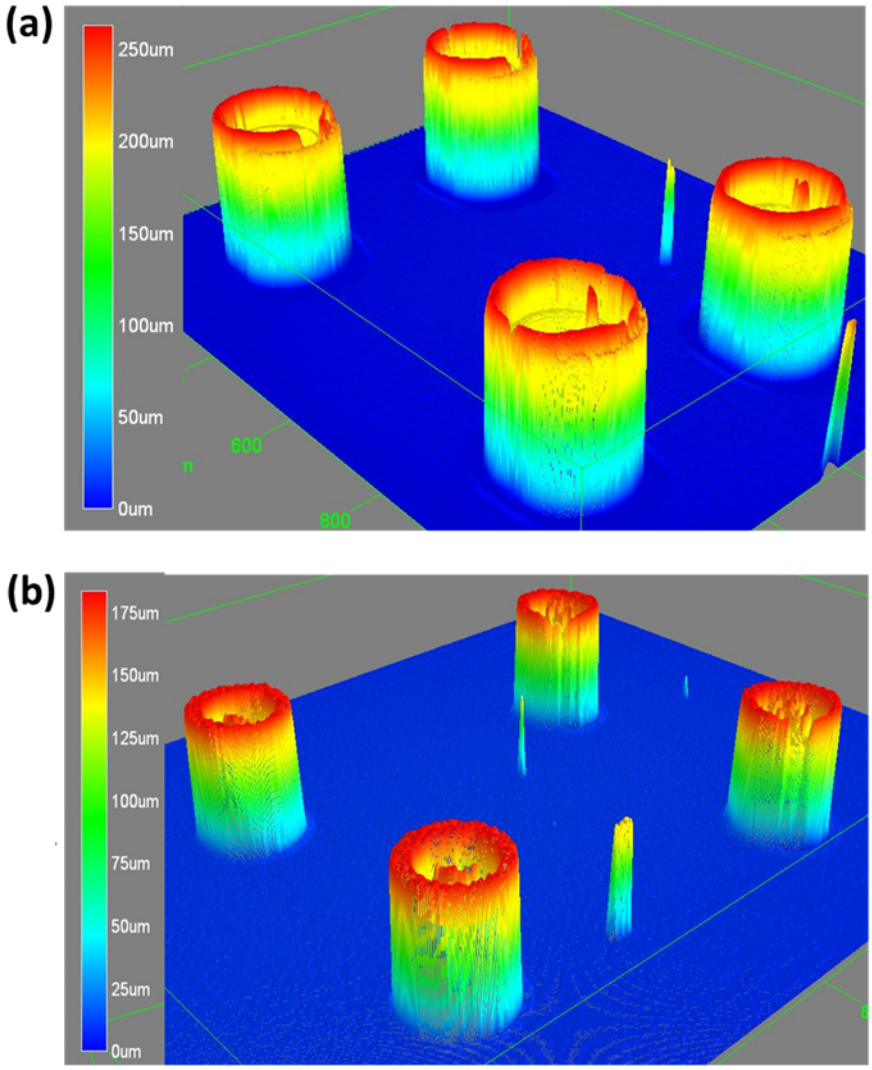

Figure 7: 3D Optical Images of Hollow Microstructures. (**a**) Before and (**b**) after pyrolysis. Reproduced with permission from refernce[24]. Copyright 2016, The Electrochemical Society. Please click here to view a larger version of this figure.

Element	Before pyrolysis	After pyrolysis
	Atomic %	Atomic %
Carbon	66.57	80.84
Oxygen	16.19	14.83
Nitrogen	7.94	0
Sulfur	9.14	0.21
Calcium	0.16	0.21
Sodium	0	0.22
Silicon	1.82	3.69

Table 1: Chemical Composition Analyzed by EDX for Human Hair Before and After Pyrolysis. Reproduced with permission from reference[13]. Copyright 2016, Elsevier Ltd.

Discussion

In this paper the methods for manufacturing a variety of carbon microstructures based on the pyrolysis of natural precursor materials or photo-patterned polymer structures were reported. The carbon materials resulting from both the traditional and non-conventional C-MEMS/C-NEMS processes are typically found to be glassy carbons. Glassy carbon is a widely used electrode material for electrochemistry and also for high-temperature applications. The microstructure of glassy carbon is composed of both crystalline and amorphous regions. Glassy carbon has high

conductivity, good resistance to high temperatures, low density, low electrical resistance, and relatively high hardness and high resistance to chemical attack.

We proposed a simple and low-cost method to fabricate hollow glassy carbon microfibers from human hair and described their application to the electrochemical sensing of ascorbic acid and dopamine. The manufacturing of long, hollow, and electrically conductive carbon microfibers was possible with the low-cost, one-step thermal treatment of human hair, which is a waste material. A human hair composed of medulla, cortex, and cuticle, produced a hollow carbon fiber after pyrolysis. The medulla disappeared, whereas the cuticle and cortex combined together and create long, hollow carbon fibers. The unique anatomy of human hair, particularly its hollow structure after pyrolysis, is characterized by a significant increase in surface area, leading to their use in electrochemical sensing. For the working electrode modified with the hair-derived carbons, the peak potentials for dopamine and ascorbic acid were shifted towards more negative and positive values respectively. The surface of the hair-derived carbon is little negatively charged which attracs positively charged dopamine and therefore, the peak currents were increased for dopamine and decreased for ascorbic acid. As a result, human hair-derived hollow carbon microfibers could be useful to detect dopamine in the presence of ascorbic acid. A comparative study of electrochemical sensing performance of bare electrodes and modified electrodes (with hair-derived carbon and CNTs) has been carried out . The hair-derived carbon modified electrode shows better sensing performance than the unmodified electrode, but the CNT-coated electrodes showed the best performance for sensing dopamine and ascorbic acid in these experimental conditions, as was expected. The CNTs shows higher sensitivity due to their greater surface-area-to-volume ratio over hair-derived hollow carbon fibers. However, the major advantage of using hair-derived carbon microfibers over CNTs is the extremely low cost. Ease of fabrication of the hair-derived carbons also makes them dominate over CNTs. It is possible to enhance the sensing performance by further modification or functionalization of the human hairs before or after pyrolysis.

The shrinkage effect due to the pyrolysis is unavoidable, as non-carbon atoms detach from the carbon bonds at high temperatures, causing a substantial loss of mass. Before designing a desired structure, one should have a good estimate off the expected shrinkage of the patterned structure. Here, the shrinkage of the carbon structures fabricated using a conventional C-MEMS process, which includes two steps for the photo-patterning and pyrolysis of polymer structures, was studied. Five strucutres with different inner diameters (0, 30, 50, 75, and 100 µm) were considered for the shrinkage study, whereas the outer diameter was kept constant at 150 µm for all structures. The structures with inner diameters of 0, 30, 50, and 75 µm showed more shrinkage on the outer diameter than the inner diameter after pyrolysis. In these cases, the outer surface areas were larger than the inner surface areas. Thus, the outer surfaces were dominant during the shrinking process, allowing more non-carbon atoms to leave the structures. In the structure with a 100 µm inner diameter, where the inner surface area also made up a significant portion of the total surface area, the shrinkage ocurred at both the inner and the outer surfaces.

The parameters for pyrolysis, such as the pyrolysis time, the maximum pyrolysis temperature, and the atmospheric environment, significantly affect the properties of the carbon structure, such as the electrical conductivity, the chemical composition, the electrochemical property, *etc.* Ongoing research focuses on revealing the effects of pyrolysis conditions on the qualities and properties of carbon structures. In the case of conventional C-MEMS, carbon structures with diverse electrical and mechanical properties can also be fabricated, resulting in a wide variety of applications, by changing the photolithography conditions, such as the baking times, the baking temperature, the type of photoresist, and the additives. It is our belief that this research can provide substantial and useful information to researchers in the field of carbon structure nano/microfabrication for a variety of applications.

Disclosures

The authors have nothing to disclose.

Acknowledgements

This work was supported by Technologico de Monterrey and the University of California at Irvine.

References

1. Wang, C., Jia, G., Taherabadi, L.H., Madou, M.J. A novel method for the fabrication of high-aspect ratio C-MEMS structures. *J Microelectromech Syst.* **14**(2), 348-58 (2005).
2. Jong, K.P.D., Geus, J.W. Carbon nanofibers: catalytic synthesis and applications. *Catal Rev Sci Eng.* **42**, 481-510 (2000).
3. Elrouby, M. Electrochemical applications of carbon nanotube. *J Nano Adv Mat.* **1**(1), 23-38 (2013).
4. Baughman, R.H., Zakhidov, A.A., Heer, W.A.D. Carbon nanotubes-the route toward applications. *Science.* **297**, 787-92 (2002).
5. Kumar, R., Singh, R.K., Singh, D.P. Natural and waste hydrocarbon precursors for the synthesis of carbon based nanomaterials: graphene and CNTs. *Renew Sustain Energy Rev.* **58**, 976-1006 (2016).
6. Afre, R.A., Soga, T., Jimbo, T., Kumar, M., Ando, Y., Sharon, M. Carbon nanotubes by spray pyrolysis of turpentine oil at different temperatures and their studies. *Micropor Mesopor Mater.* **96**(1-3), 184-90 (2006).
7. Sharma, S., Kalita, G., Hirano, R., Hayashi, Y., Tanemura, M. Influence of gas composition on the formation of graphene domain synthesized from camphor. *Mater Lett.* **93**(0), 258-62 (2013).
8. Ghosh, P., Afre, R.A., Soga, T., Jimbo, T. A simple method of producing single-walled carbon nanotubes from a natural precursor: eucalyptus oil. *Mater Lett.* **61**(17), 3768-70 (2007).
9. Kumar, R., Tiwari, R., Srivastava, O. Scalable synthesis of aligned carbon nanotubes bundles using green natural precursor: neem oil. *Nanoscale Res Lett.* **6**(1), 92-97 (2011).
10. Liang, Y., Wu, D., Fu, R. Carbon microfibers with hierarchical porous structure from electrospun fiber-like natural biopolymer. *Sci Rep.* **3**, 1-5 (2013).
11. Gupta, A. Human hair "waste" and its utilization: gaps and possibilities. *J Waste Manag.* **2014**, 1-17 (2014).

12. Qian, W., Sun, F., Xu, Y., Qiu, L., Liu, C., Wang, S., Yan, F. Human hair-derived carbon flakes for electrochemical supercapacitors. *Energy Environ Sci.* **7**, 379-86 (2014).
13. Pramanick, B., Cadenas, L.B., Kim, D.M., Lee, W., Shim, Y.B., Martinez-Chapa, S.O., Madou, M.J., Hwang, H. Human hair-derived hollow carbon microfibers for electrochemical sensing. *Carbon.* **107**, 872-877 (2016).
14. Miura, N., Numaguchi, T., Yamada, A., Konagai, M., Shirakashi, J. Room temperature operation of amorphous carbon-based single-electron transistors fabricated by beam-induced deposition techniques. *Jpn J Appl Phys.* **37**(2), L423-25 (1998).
15. Irie, M., Endo, S., Wang, C.L., Ito, T. Fabrication and properties of lateral p-i-p structures using single crystalline CVD diamond layers for high electric field applications. *Diamond Rel Mater.* **12**, 1563-68 (2003).
16. Tay, B.K., Sheeja, D., Yu, L.J. On stress reduction of tetrahedral amorphous carbon films for moving mechanical assemblies. *Diamond Rel Mater.* **12**, 185-94 (2003).
17. Kamath, R.R., Madou, M.J. Three-dimensional carbon interdigitated electrode arrays for redox-amplification. *Anal Chem.* **86**(6), 2963-71 (2014).
18. Sharma, S., Khalajhedayati, A., Rupert, T.J., Madou, M.J. SU8 derived glassy carbon for lithium ion batteries. *ECS Trans.* **61**(7), 75-84 (2014).
19. Kim, D., Pramanick, B., Salazar, A., Tcho, I.-W., Madou, M.J., Jung, E.S., Choi, Y.-K., Hwang, H. 3D carbon electrode based triboelectric nanogenerator. *Adv Mater Technol.* **1**(8), 1-7 (2016).
20. Duarte, R.M., Gorkin,R.A., Samra, K.B., Madou, M.J. The integration of 3D carbon-electrode dielectrophoresis on a CD-like centrifugal microfluidic platform. *Lab Chip.* **10**, 1030-43 (2010).
21. Mund, K., Richter, G., Weidlich, E., Fahlstrom, U. Electrochemical properties of platinum, glassy carbon, and pyrographite as stimulating electrodes. *Pacing Clin Electrophysiol.* **9**(6), 1225-29 (1986).
22. Xua, H., Malladi, K., Wang, C., Kulinsky, L., Song, M., Madou, M. Carbon post-microarrays for glucose sensors. *Biosens Bioelectron.* **23**, 1637-44 (2008).
23. Sharma, S., Madou, M. Micro and nano patterning of carbon electrodes for bioMEMS. *Bioinspir Biomim Nanobiomat.* **1**(BBN4), 252-65 (2012).
24. Pramanick, B., Martinez-Chapa, S.O., Madou, M. Fabrication of biocompatible hollow microneedles using the C-MEMS process for transdermal drug delivery, *ECS Trans.* **72**(1), 45-50 (2016).

